Photoreduction of nitrogen and water on montmorillonite clays loaded with hydrous ferric oxide

O. A. Ileperuma[1], W. C. B. Kiridena and W. D. D. P. Dissanayake
Institute of Fundamental Studies, Kandy (Sri Lanka)

(Received September 18, 1990; in revised form January 15, 1991)

Abstract

Montmorillonite clays with interlamellar cations replaced by oligomeric hydrous ferric oxides convert nitrogen to NH_3 and H_2O to hydrogen with higher efficiencies than hydrous ferric oxide alone. The enhanced activity is attributed to the larger surface area presented by the clay and to the retardation of NH_3 photo-oxidation.

1. Introduction

Clays are a class of stable aluminosilicate materials which readily disperse in water, possess large surface areas and catalytic activity [1, 2]. The montmorillonite clays, in particular, exhibit the ability to form pillared compounds when the interlamellar cations in the clay are replaced with bulky polymeric inorganic cations followed by calcination. Such pillared clays have applications as industrial catalysts [1] in the petroleum industry. Semiconductors such as ZnS and CdS when loaded onto montmorillonite suspensions photogenerate hydrogen [3] in the presence of a sacrificial donor.

The photoreductions of nitrogen to NH_3 and H_2O to hydrogen on semiconductor-based catalysts have been studied [4] as possible means of solar energy conversion to give useful products. However, the quantum efficiencies reported for such processes are too low to be of any practical value. Furthermore, in the photoreduction of nitrogen, the yields of NH_3 reach a maximum at about 1–2 h followed by a decrease in catalytic activity. This arises due to competing reactions, such as the photo-oxidation of the NH_3 formed, and catalyst poisoning. We have previously reported [5] the photoreduction of nitrogen to NH_3 on hydrous ferric oxide using visible light. Here, the catalytic activity is due to the strongly negative flat band potential and the strong chemisorption of nitrogen on the small hydrous oxide particles. However, even with this catalyst, the NH_3 yields decrease during long-term irradiation. It has also been observed [6] that partial loading of the ferric oxide with Ti^{IV} results in enhanced yields of NH_3 with no nitrate observed up to 12 h of irradiation. Here, the possible separation of active sites for hydrogen and oxygen evolution has been suggested as the reason for the enhanced NH_3 yields obtained. A similar effect is observed when montmorillonite clays such as bentonite are loaded with hydrous forms of ferric oxides to form precursor pillared clays. Furthermore, such catalysts are also active for photogenerating hydrogen from H_2O under non-sacrificial conditions.

[1]Also at: Department of Chemistry, University of Peradeniya, Peradeniya, Sri Lanka.

1010-6030/91/$3.50

2. Experimental details

2.1. Preparation of catalysts

Bentonite (BDH grade) was suspended in water and the supernatant suspension was separated from the heavier fraction. This suspension was centrifuged for 1 h at 2000 rev min^{-1} and warmed with Al–NaOH to remove all traces of NH_4^+, NO_2^- and NO_3^-. The resulting solid was then thoroughly washed with dilute acid and deionized water. The analytical grade reagents employed were also purified in a similar manner. Iron-loaded bentonite clays were prepared by two different methods. In method (a), a sol form of colloidal Fe^{III} hydroxo complexes was prepared and loaded onto bentonite; in method (b), ferric ions adsorbed onto bentonite were converted to hydrous ferric oxide.

(a) A portion of 10 ml of 0.2 M $FeCl_3$ solution was stirred at 80 °C, followed by the slow addition of a solution of 0.2 M NaOH until the molar ratio of $FeCl_3$ to NaOH reached a value of 1:2.5. This resulted in the formation of a wine red solution which is presumed to be polymeric Fe^{III} hydroxo species. This solution was added to 100 mg of the purified clay and stirred overnight. At this stage all the iron in the solution was adsorbed onto the clay. The precipitate obtained was separated by centrifuging and washed several times with deionized water until there was no trace of NH_4^+, NO_3^- or Cl^- in the washings.

(b) Clay-supported hydrous ferric oxide catalysts were prepared in a slightly different manner. A suspension containing 5 g of the purified bentonite clay in 200 ml of 0.1 M $FeCl_3$ was stirred for 24 h. The resultant Fe^{3+}-exchanged clay was then treated with an excess of 0.1 M NaOH. The solid obtained was separated by centrifugation and washed thoroughly with distilled water. Since these catalysts lose their activity on drying, they were stored under water.

2.2. Irradiation procedure

Iron-loaded bentonite clay catalysts (200 mg) were suspended in 100 ml of double-distilled water in an Applied Photophysics immersion well photochemical reactor of 125 ml capacity. The lamp used was a 125 W medium pressure mercury arc lamp housed inside a water-cooled quartz jacket. The lamp emits more than 7×10^{18} photons s^{-1} cm^{-2} inside the reaction flask. Irradiation was carried out under a stream of purified nitrogen (hot copper pellet column, chromic acid solution, potassium hydroxide and water). After irradiation, the mixture was distilled with 20 ml of 0.2 M NaOH and the ammonia in the distillate was determined by the indophenol blue method [7]. A portion of the catalyst suspension after irradiation was centrifuged and the nitrate content in the clear supernatant liquid was determined colorimetrically by the coupling reaction of sulphanilic acid and *N*-(1-naphthyl)ethylenediamine after cadmium reduction. Control experiments were carried out in the dark with nitrogen purging and the level of ammonia obtained here was taken as the zero standard. Control experiments carried out under argon with irradiation showed no detectable traces of NH_3 and NO_3^- under identical experimental conditions.

2.3. Hydrogen evolution experiments

Hydrogen evolution during photolysis under both nitrogen and argon was determined by gas chromatography (Shimadzu GC-9AM gas chromatograph, molecular sieve column and argon carrier gas). These experiments were independently checked by carrying out photolysis in a reaction vessel equipped with a polarographic detector (Applied Photophysics). Oxygen evolution was also tested using the same procedure.

2.4. Characterization of the catalysts

Electrochemical measurements were carried out using a Hokuto–Denko potentiostat model HA 301. This instrument was connected to a three electrode assembly consisting of a working electrode (photoanode), a saturated calomel electrode (SCE) as the reference electrode and a platinum counter electrode. The photoanode was prepared by pressing the catalyst into a fibre glass disc. A quartz cell was used to perform the photoelectrochemical experiments and a tungsten bulb (100 W) was used as the illumination source. The cell was protected from stray light and the dark current was adjusted to zero. The photocurrent generated under continuous light chopping was biased by an externally applied potential until there was no change in the photocurrent during light chopping. The value of the externally applied voltage was then taken as the flat band potential under the particular conditions of the electrolyte employed.

X-ray powder diffraction patterns of the clay catalysts were obtained on a Shimadzu model XD-7A diffractometer using Cu Kα radiation. The particle size distributions of the catalysts were obtained with a Horiba model CAPA-700 particle size analyser using the sedimentation technique.

3. Results and discussion

3.1. Characterization of the catalysts

The wine red solution obtained by the hydrolysis of $FeCl_3$ is presumed to contain polymeric Fe^{III} hydroxo complexes with the predominant form being a dimer. When these solutions are treated with clays such as bentonite, precursors to their pillared forms are obtained. The average particle size for the bentonite precursor pillared clay with iron hydroxo species is about 0.66 μm in diameter. The X-ray diffraction patterns recorded for a clay film at 303 K exhibit a prominent peak in the region $2\theta < 10$. For bentonite this reflection (001) corresponds to a basal spacing of $d_{001} = 12.44$ Å allowing only one water monolayer intercalated between clay sheets. For the clay containing intercalated polymeric iron hydroxo species, the d_{001} spacing is 15.49 Å corresponding to two water monolayers.

The absorption spectrum of the hydrated ferric oxide was measured by reflection and exhibits an absorption threshold at approximately 595 nm corresponding to an energy gap of approximately 2.1 eV. The bentonite containing intercalated polymeric iron hydroxo species has an absorption threshold at 520 nm, which corresponds to an energy gap of 2.38 eV (Fig. 1). A similar observation has been reported by Bard [8] where the absorption edge of CdS is shifted towards the UV region on intercalation to montmorillonite clays.

Anodic photocurrents produced by the illumination of the catalyst electrode were collected by a platinum flag as described in Section 2.4. In all these experiments, potential shifts occur in the negative direction with reference to SCE. The flat band potential values become more negative with increasing pH (Fig. 2). This is similar to the shifts observed for hydrous ferric oxide which has a flat band potential of -0.34 V (*vs.* a normal hydrogen electrode (NHE)) at pH 11 [9]. Under these conditions, the position of the conduction band of α-Fe_2O_3, which is normally thermodynamically unsuited for hydrogen generation, becomes sufficiently negative for the photogeneration of hydrogen from H_2O [5, 9].

3.2. Photoreduction of nitrogen

The montmorillonite clays, such as bentonite, can be readily dispersed in water, possess large surface areas (approximately 750 $m^2\ g^{-1}$) with a very high cation exchange

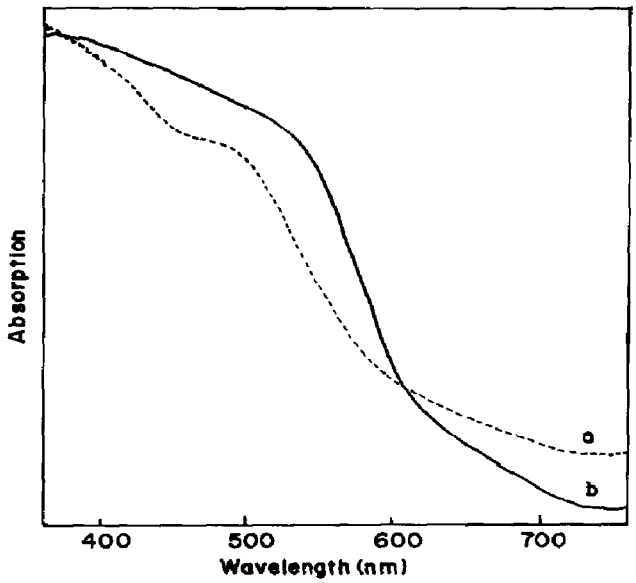

Fig. 1. Reflectance spectra of (a) polymeric iron hydroxo species adsorbed onto bentonite and (b) after heating at 250 °C for 4 h to give the pillared form.

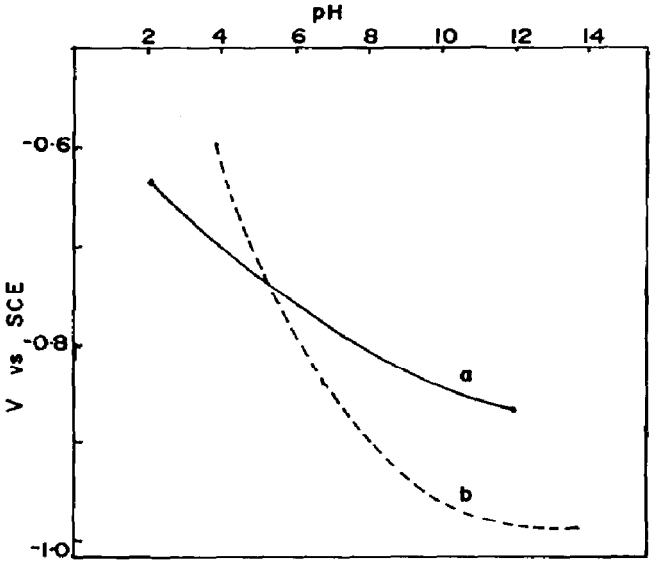

Fig. 2. Variation in the flat band potential values (*vs.* SCE) with pH of the catalysts: (a) polymeric iron hydroxo species adsorbed onto bentonite; (b) hydrous ferric oxide.

capacity (approximately 100 mequiv. per 100 g) and exhibit unusual intercalation and swelling properties [10]. These properties seem to be particularly advantageous for the preparation of efficient semiconductor-based catalyst systems. Furthermore, since bentonite is a phyllosilicate having a sheet-like structure with a negatively charged surface [11], the separation of charge carriers photogenerated on the hydrous ferric oxide may be possible. This could generate separate sites for photoreduction of nitrogen

and for photo-oxidation, thereby preventing oxidation of NH_3 to NO_3^- which is detrimental to the catalytic activity of this system [5].

Figure 3 shows the yield of ammonia and nitrate from the catalysts hydrous ferric oxide, bentonite loaded with hydrous ferric oxide and precursor pillared bentonite loaded with polymeric iron hydroxo complex at pH 10. The optimum NH_3 yields are obtained at this pH value. A feature common to all catalysts is that the NH_3 concentration in the solution rapidly increases, reaches a maximum value after 4–6 h and then gradually decreases. This decrease is followed by a concomitant slow increase in NO_3^- concentration. It is clearly seen that the NH_3 concentration for the iron-loaded bentonite systems shows an enhancement by a factor of about three. In addition, the maximum yield of NH_3 is reached after 1 h for hydrous ferric oxide, whereas for bentonite–Fe_2O_3 this period is 6 h. In the latter case NO_3^- formation appears only after 6 h. This observation supports the hypothesis that NO_3^- formation inhibits the photosynthesis of NH_3. The formation of NH_3 can be expressed by reactions (1)–(4). The quantum yields observed for NH_3 formation are in the range 0.01%–0.02%.

$$Fe_2O_3 \xrightarrow{h\nu} Fe_2O_3^*(h^+, e^-) \quad (1)$$

$$N_2 + 6H^+ + 6e \longrightarrow 2NH_3 \quad (2)$$

$$2H_2O + 2e \longrightarrow 2OH^- + H_2 \quad (3)$$

$$2H_2O + 4h^+ \longrightarrow O_2 + 4H^+ \quad (4)$$

In the case of water decomposition, multielectron transfer can be enhanced by loading the catalyst with noble metals such as platinum. However, platinization of the catalysts employed in this study resulted in a loss of catalytic activity.

The formation of NO_3^- on irradiation can be attributed to the oxidation of NH_3. This process most probably occurs via the participation of hydroxyl free radicals formed by the capture of photogenerated holes by adsorbed OH^- ions (reaction (5))

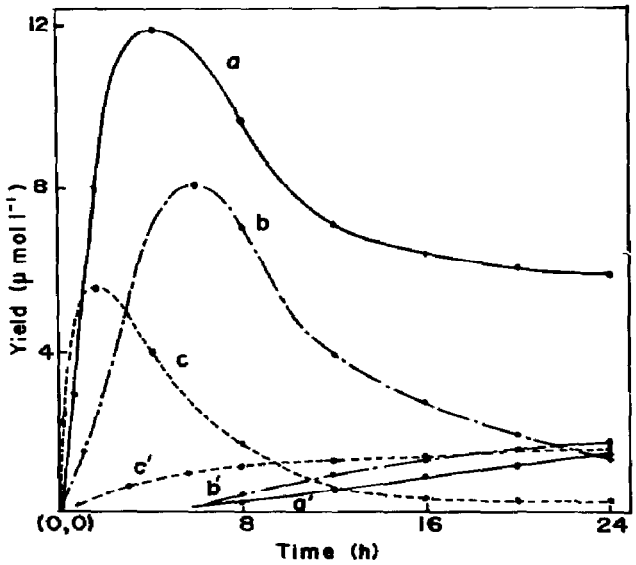

Fig. 3. Variation in ammonia (a–c) and nitrate (a'–c') yields with time for (a) polymeric iron hydroxo species adsorbed onto bentonite, (b) hydrous ferric oxide adsorbed onto bentonite and (c) hydrous ferric oxide.

$$OH^- + h^+ \longrightarrow OH \quad (5)$$

The mechanism of NH_3 oxidation by OH has been deduced by flash photolysis experiments [12] and the end product has been identified as HNO. This may further react with oxygen to yield HNO_2. The oxidation of NH_3 in solution to NO_2^- during UV irradiation in the presence of semiconductors is well established [13, 14]. In our experiments, the initial formation of both NO_2^- and O_2^{2-} was detected. However, irradiation over a longer period of time caused a gradual decrease in concentration of these species, resulting in NO_3^- as the final oxidation product. Oxidation of NO_2^- to NO_3^- could take place via the involvement of photogenerated peroxide ions. Nevertheless, the extent of NO_3^- formation is less for the Fe_2O_3-loaded bentonite systems than for hydrous ferric oxide alone.

Heating the precursor pillared clays for 2 h at 250 °C results in the formation [15] of a pillared structure of the iron oxide in the layered silicate. However, these catalysts exhibit little activity towards nitrogen reduction showing that the degree of hydration is crucial for catalytic activity.

3.3. Photogeneration of hydrogen

Figure 4 shows the yields of hydrogen obtained on irradiation (400 W mercury arc lamp) of a catalyst suspension of the bentonite precursor pillared clay containing polymeric iron hydroxo species. After 8 h, hydrogen formation is higher under nitrogen and, after 24 h, 920 μl of hydrogen are produced under nitrogen. A similar observation has been made by Schrauzer *et al.* [16] for Fe–TiO_2 catalyst and attributed to "nitrogen-stimulated hydrogen production" (reactions (6)–(8))

$$N_2 + 2e^- + 2H^+ \longrightarrow N_2H_2 \quad (6)$$

$$N_2H_2 \longrightarrow \tfrac{1}{2}N_2H_4 + \tfrac{1}{2}N_2 \quad (7)$$

$$N_2H_4 \longrightarrow N_2 + 2H_2 \quad (8)$$

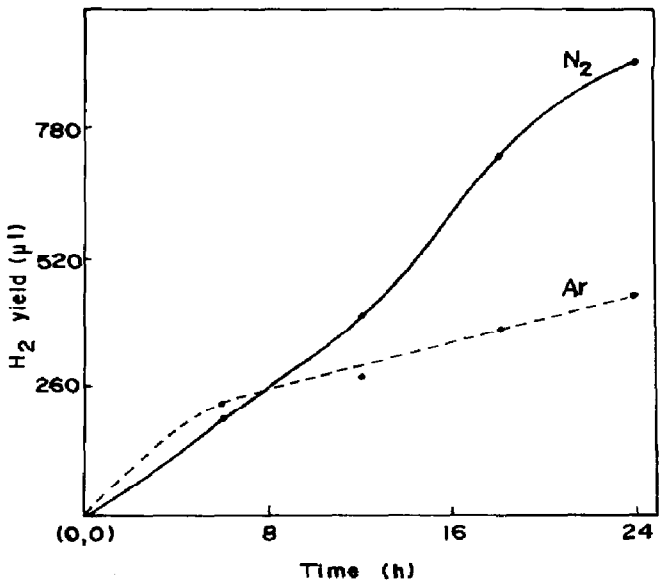

Fig. 4. Variation in hydrogen yields with time under argon and nitrogen for the bentonite catalyst containing polymeric iron hydroxo species.

Hydrogen and oxygen evolution rates were independently measured using hydrogen and oxygen electrodes and a calibrated membrane polarographic detector. Argon bubbling was carried out after each irradiation to eliminate dissolved hydrogen in the reaction medium and repeated irradiations were performed. The results show similar variations for each cycle. With the ferric oxide catalyst systems investigated, oxygen evolution is observed only after long-term irradiation. It is suggested that hydrogen peroxide is formed from OH radicals (reaction (5)) and that oxygen is formed from H_2O_2. Our results show that 3.5 μmol l^{-1} of peroxide is formed after 12 h of irradiation (colorimetric determination using I_3^- formed when these solutions are treated with acidified KI solution).

Acknowledgments

The authors thank Professors D. T. B. Tennakone and K. Tennakone for many useful discussions. Financial assistance from NARESA (Grant No. RG/87/C/2) and a PSTC grant from US AID (Grant No. 936-5542) are gratefully acknowledged.

References

1 D. E. Vaughan, R. J. Lussier and J. S. Magee, *German Patent 2, 825* (1979) 769.
2 S. Yamanaka and G. W. Brindley, *Clays Clay Miner., 27* (1979) 119.
3 O. Enea and A. J. Bard, *J. Phys. Chem., 90* (1986) 301.
4 G. N. Schrauzer and T. D. Guth, *J. Am. Chem. Soc., 99* (1977) 7189.
Q. Li, K. Domen, S. Saito, J. Onishi and K. Tamaru, *Chem. Lett.,* (1983) 321.
E. Endoh, J. K. Leland and A. J. Bard, *J. Phys. Chem., 90* (1986) 6223.
5 K. Tennakone, S. Wickremanayake, C. A. N. Fernando, O. A. Ileperuma and S. Punchihewa, *J. Chem. Soc., Chem. Commun.,* (1987) 1078.
6 K. Tennakone, C. A. N. Fernando, S. Wickramanayake, M. W. P. Damayanthi, L. H. K. de Silva, W. Wijeratne, O. A. Ileperuma and S. Punchihewa, *Sol. Energ. Mater., 17* (1987) 47.
7 D. F. Boltz and J. A. Howell, *Colorimetric Determination of Nonmetals,* Wiley, New York, 1978.
8 A. J. Bard, *Ber. Bunsenges. Phys. Chem., 92* (1988) 1187.
9 J. Kim and M. Graetzal, *J. Chem. Soc., Faraday Trans. 1, 83* (1987) 1101.
10 H. Van Damme, H. Nijs and J. M. Fripiat, *J. Mol. Catal., 27* (1984) 123.
11 H. Van Ophen, in *An Introduction to Clay Chemistry,* Wiley, New York, 1977, p. 566.
12 H. Mozzanega, J. M. Herrmann and P. Pichat, *J. Phys. Chem., 83* (1979) 2251.
13 J. C. McConnell, *J. Geophys. Res., 78* (1973) 7812.
14 W. Maclean and M. Ritchie, *J. Appl. Chem., 45* (1965) 452.
15 D. T. B. Tennakone, W. Jones and J. M. Thomas, *Solid State Ionics, 24* (1987) 205.
16 G. N. Schrauzer, T. D. Guth, J. Salehi, N. Strampach, L. N. Hui and M. R. Palmer, in E. Pelizetti and N. Serpone (eds.), *Homogeneous and Heterogeneous Photocatalysis,* Reidel, New York, 1986, p. 509.